

Accepted Manuscript

Title: Stability or Flexibility: Metal Nanoparticles Supported over Cross-linked Functional Polymers as Catalytic Active Sites for Hydrogenation and Carbonylation

Author: Bingfeng Chen Fengbo Li Zhijun Huang Tao Lu Guoqing Yuan



PII: S0926-860X(14)00311-1
DOI: <http://dx.doi.org/doi:10.1016/j.apcata.2014.05.001>
Reference: APCATA 14820

To appear in: *Applied Catalysis A: General*

Received date: 4-11-2013
Revised date: 13-4-2014
Accepted date: 1-5-2014

Please cite this article as: B. Chen, F. Li, Z. Huang, T. Lu, G. Yuan, Stability or Flexibility: Metal Nanoparticles Supported over Cross-linked Functional Polymers as Catalytic Active Sites for Hydrogenation and Carbonylation, *Applied Catalysis A, General* (2014), <http://dx.doi.org/10.1016/j.apcata.2014.05.001>

This is a PDF file of an unedited manuscript that has been accepted for publication. As a service to our customers we are providing this early version of the manuscript. The manuscript will undergo copyediting, typesetting, and review of the resulting proof before it is published in its final form. Please note that during the production process errors may be discovered which could affect the content, and all legal disclaimers that apply to the journal pertain.

**Stability or Flexibility: Metal Nanoparticles Supported over
Cross-linked Functional Polymers as Catalytic Active Sites
for Hydrogenation and Carbonylation**

Bingfeng Chen^a, Fengbo Li^{*a}, Zhijun Huang^a, Tao Lu^{a,b}, Guoqing Yuan^{*a}

^a Beijing National Laboratory of Molecular Science, Key Laboratory of Green Printing, Institute of Chemistry, Chinese Academy of Sciences, Beijing, 100190, P. R. China; Tel : (86) -10-62634920; Fax: (86) -10-62559373; E-mail: lifb@iccas.ac.cn; yuangq@iccas.ac.cn

^b University of Chinese Academy of Sciences, Beijing, 100049, P. R. China

Abstract

A novel cross-linked functional polymer was prepared through copolymerization between 1, 3, 4, 6-tetraallylglycoluril and 4-vinyl pyridine. Pt and Pd nanoparticles supported over this polymeric framework (Pt/CFP and Pd/CFP) were detailedly characterized by TEM, EDS, and XPS. Pt nanoparticles were kept in the monodispersed state with the average size of 1.4 nm. Monodispersed Pd nanoparticles were about 4.5 nm. The hydrogenation of nitrobenzenes over Pt/CFP shows high activity and selectivity with the substrate to Pt ratio of 4000 under mild reaction reactions. Pd/CFP was the catalyst for carbonylation of aryl iodides in the presence of secondary amines and acylhydrazines. Double carbonylation with secondary amines produced α -ketoamides with the selectivity of 80%. Diacylhydrazine molecules were synthesized by the direct carbonylation of aryl iodide with acylhydrazine over Pd/CFP. The recyclability and recoverability of Pt/CFP were investigated through a seven-run recycling test of nitrobenzene hydrogenation. The flexibility of Pd/CFP in the carbonylation process was thoroughly explored by a twelve-run recycling test. Supported Pt or Pd nanoparticles showed the macroscopic robustness in their catalytic performance in the catalytic cycle. The flexibility of metal nanoparticles and the polymeric supports guaranteed macroscopic catalytic robustness.

Keywords: Functional polymer; Metal nanoparticles; Hydrogenation; Carbonylation; Recoverability and recyclability.

1. Introduction

Most of the industrial catalysts are made of metal or metal oxide particles of a few nanometers in size and the reaction proceeds at the molecular scale. Nanocatalysis is the intrinsic property of the catalyst. Supported metal nanoparticles constitute the majority of the heterogeneous catalysts and show catalytic properties different from small atom clusters or the bulk crystal surfaces. Gold is the most famous model system [1]. The size-dependence effect is the specialty of catalysis over metal nanoparticles [2, 3]. First, metal nanoparticles have irregular surfaces with abundant structural defects on the steps and kinks, which are favorable low-coordinated sites for the breaking and forming of chemical bonds [4, 5]. Second, metal nanoparticles' surface offers the flexibility of structure recovering in the adsorption and desorption of the catalytic reaction. The third property, which influences catalysis, is the electronic structure of metal nanoparticles [6, 7].

Metal nanoparticles are excellent catalysts for chemical synthesis [8-10]. However, active nanoparticles are not stable and show a high tendency toward agglomeration, which then leads to deactivation and precipitation. Protecting agents to stabilize metal nanoparticles include various materials, such as metal oxide [11, 12], carbon materials [13], porous silica [14] and polymers [15, 16]. The flexibility of metal nanoparticles is necessary for active catalytic performance. However, it results in their instability during the catalytic reaction. (One sentence was deleted.)

Metal nanoparticles bridge the gap between homogeneous and heterogeneous catalysis. Some metal nanoparticles with stabilizing agents are soluble in the reaction

medium as homogeneous catalysis. On the other hand, metal nanoparticles have an active surface as heterogeneous catalysis. However, it is a major challenge to separate the catalyst from the reaction mixture. In our previous researches [17, 18], cross-linked functional polymers (CFPs) were demonstrated to be excellent supports for metal nanoparticle catalysts to be employed in the liquid phase. The swelling behavior of the polymer support facilitates the dispersion of metal nanoparticle precursors in the polymeric framework, which are further immobilized by the functional groups. Under liquid-phase conditions, the formation of swollen-gel phase is favorable for the involvement of all reactants in the catalytic reaction.

CFPs supported metal nanoclusters had been applied in commercial production of MIBK from acetone and hydrogen in 1965 [19]. EnCat catalyst by Reaxa was another commercial catalyst based on polyurea supported palladium [20]. Typical CFPs consist of three components: chemical structure, cross-linked, and functional groups. Chemical structures are the main polymer chain such as poly-DMA, polyacrylate, poly-MMA, and PS. The most employed cross-linkers are DVB and MBAA. Functional groups are used to anchor metal nanoparticles' precursors. There are two types of attachment strategies: ion-pair interaction ($-\text{SO}_3^-$, COO^- and $-\text{NR}^{3+}$) and chelating interaction (Lewis base groups: amino, pyridyl, benzimidazolyl, thiol, methylsulfide, and nitrile) [21-24]. Supported metal species are mostly noble metals, such as Pt, Pd, Ru, Rh, and Au [25, 26]. (One sentence was deleted.) There are three methods to prepare CFPs supported metal nanoparticles: 1) introduction of a suitable metal precursor into CFPs and generation of metal nanoparticles through reduction or

decomposition of the precursor (RIMP), 2) incorporation of metal precursors into CFPs during the polymerization and generation of metal nanoparticles through reduction or decomposition of the precursor (IMPR), 3) direct introduction of prepared metal nanoparticles into CFPs (IPMN) [27]. Kobayashi et al. have reported “polymer-microencapsulated catalysts” and “polymer-incarcerated catalysts”, which provide new insights into the preparation and catalytic application of polymer-supported metal nanoparticles [28-30]. Recently, Yamada et al. have found a novel CFPs-supported metal nanocluster catalyst: self-assembled poly (imidazole-palladium) exhibits high catalytic activity and excellent resuability in several C-C formation reactions [31]. The aim of these proposed strategies is to achieve high catalytic activity with good recoverability and recyclability.

In this work, a new cross-linker based on glycoluril [32, 33] was synthesized and then copolymerized with 4-vinyl pyridine to produce cross-linked functional polymeric support for metal nanoparticles. Pt and Pd nanoparticles over this CFP were prepared and their catalytic properties in hydrogenation and carbonylation were further investigated. The catalytic behavior and transform of supported metal nanoparticles during the reaction were explored to interpret the structure-property relation.

2. Experimental

2.1 Preparation of 1, 3, 4, 6-tetraallylglycoluril

A three-neck 100 ml flask was flushed with argon. Anhydrous DMSO (40 ml) was

added and glycoluril (1.42 g, 10 mmol) was dissolved. Then potassium tert-butoxide (5.62 g, 50 mmol) was gradually added and the mixture was further stirred for 1.0 h. Allyl bromide (7.0 ml, 80 mmol) was injected into the reaction mixture and the reaction was performed at 25 °C for 20 h. 500 ml aqueous solution of HCl (0.1 M) was added into the reaction mixture. 100 ml ethyl acetate was used to extract the mixture and the organic phase was washed by saturated NaCl aqueous solution (100 ml) for three times. After being dried by MgSO₄, the solvent was removed. 1.53 g target product was obtained after purification over silica column with the eluent of ethyl acetate/ petroleum ether (60-90 °C) (v/v, 3:2). All procedures were performed in argon atmosphere.

2.2 Preparation of cross-linked functional polymer (CFP)

The copolymerization was performed in a 100-ml two-neck flask under argon flow. 1, 3, 4, 6-tetraallylglycoluril (1.51 g, 5 mmol) and 4-vinyl pyridine (1.07 ml, 10 mmol) were dissolved in 20 ml anhydrous toluene. Azobisisobutyronitrile (164 mg, 0.05 mol/L) was used as the radical initiator and the polymerization proceeded at 60 °C for 21 h. The resulting solid materials were filtered and extracted by petroleum ether for three times. After being dried under vacuum, yellow solid (0.89 g) was obtained.

2.3 Preparation of Pt/CFP and Pd/CFP

CFP (250 mg) was fully swollen in 30 ml anhydrous ethanol. And then K₂PtCl₄ (28 mg, 0.0674 mmol) was added. The mixture was further stirred at room temperature for 20 h. NaBH₄ (25.5 mg, 0.674 mmol) in 6.0 ml water was injected and the reduction proceeded for 3.0 h. Finally, a 100 ml mixture of petroleum ether and

diethyl ether was added into the mixture and the resulting precipitate was collected. After being dried under vacuum, brown solid (Pt/CFP, 216 mg) was obtained. Pt/CFP (50 mg) was calcined in air at 600 °C for 3 h. The final ash was dissolved in mixture HNO₃ and HCl aqueous solution (4.0 ml). The solution was diluted to 100 ml with dionized water. The Pt concentration was determined by ICP-AES. The calculated Pt load of Pt/CFP was 2.02 wt%.

CFP (400 mg) was fully swollen in 50 ml anhydrous ethanol. And then PdCl₂(CH₃CN)₂ (70 mg, 0.27 mmol) was added. The mixture was further stirred at room temperature for 20 h. NaBH₄ (70 mg, 1.85 mmol) in 16 ml water was injected and the reduction proceeded for 3.0 h. Finally, a 150 ml mixture of petroleum ether and diethyl ether was added into the mixture and the resulting precipitate was collected. After being dried under vacuum, deep gray solid (Pd/CFP, 392 mg) was obtained. Pd/CFP (50 mg) was calcined in air at 600 °C for 3 h. The final ash was dissolved in mixture HNO₃ and HCl aqueous solution (4.0 ml). The solution was diluted to 100 ml with dionized water. The Pd concentration was determined by ICP-AES. The calculated Pd load of Pd/CFP was 1.10 wt%.

2.4 Hydrogenation of nitrobenzenes over Pt/CFP

To a 10-ml Schlenk tube, were added nitrobenzene (1.0 mmol), THF (2.0 ml) and the catalyst (S/Pt: 4000). The Schlenk tube was flushed by hydrogen flow and then directly connected to a hydrogen balloon (1.0 atm). After the given reaction time, the catalyst was separated by simple filtration. The reaction results were determined by GC. In the seven-run recycling test, the catalyst was separated by filtration and

washed by ethyl acetate and diethyl ether after each testing run. The catalyst was dried vacuum and then recycled into the next batch.

2.5 Carbonylation of aryl iodide in the presence of secondary amines over Pd/CFP

To a 100-ml autoclave, were added aryl iodide (1.0 mmol), secondary amine (5.0 mmol), the catalyst (Pd: 0.78 mol%), Cs_2CO_3 (1.14 g, 3.5 mmol), LiI (9.0 mg, 0.0479 mmol) and toluene (5.0 ml). The autoclave was flushed by CO flow and pressurized to 4.0 MPa. The reaction was performed at 120 °C for the given time. The reaction mixture was extracted with ethyl acetate. Double carbonylation and mono carbonylation products were obtained by purification over silica column with the eluent of ethyl acetate/ petroleum ether (60-90 °C) (v/v, 1:4). In the twelve-run recycling test, the catalyst was separated by filtration and washed sequentially by water, ethyl acetate and diethyl ether after each testing run. The catalyst was dried vacuum and then recycled into the next batch.

2.6 Carbonylation of aryl iodide in the presence of acylhydrazines over Pd/CFP

To a 100-ml autoclave, were added aryl iodide (1.0 mmol), acylhydrazine (2.0 mmol), the catalyst (Pd: 0.78 mol%), base (1.06 mmol) and DMSO (5.0 ml). The autoclave was flushed by CO flow and pressurized to 4.0 MPa. The reaction was performed at 120 °C for the given time. The reaction mixture was extracted with ethyl acetate. The carbonylation product was obtained by purification over silica column with the eluent of ethyl acetate/ petroleum ether (60-90 °C) (v/v, 2:1). In the five-run recycling test, the catalyst was separated by adding 30 ml mixture of petroleum ether and diethyl ether and washed by ethyl acetate and diethyl ether after each testing run. The catalyst

was dried vacuum and then recycled into the next batch.

2.7 Materials characterization

X-ray photoelectron spectroscopy data were obtained with an ESCALab220i-XL electron spectrometer from VG Scientific using 300W Al-K α radiation. The base pressure was about 3×10^{-9} mbar. The binding energies were referenced to the C1s line at 284.8 eV from adventitious carbon. Eclipse V2.1 data analysis software supplied by the VG ESCA-Lab200I-XL instrument manufacturer was applied in manipulation of the acquired spectra. Transmission electron microscopy (TEM) and EDS were obtained by a JEOL 2010 TEM with an accelerating voltage of 200 kV. FTIR was performed over Bruker TENSOR-27. Gel Permeation Chromatography (GPC) was carried out by Water 1515 with the solvent of DMF. Thermal gravimetric analysis was performed over STA 409PC. ICP-AES was performed by Perkin Elmer Optima 5300 dv. GC was carried out over GC-2014 (SHIMADZU) with high temperature capillary column (MXT-1, 30m, 0.25mm ID) and FID detector.

Silica gel (200-300 mesh) was used for column chromatography. Melting points were recorded on an uncorrected Melting Point X-4 instrument. ^1H NMR and ^{13}C NMR spectra were recorded on a 400 MHz spectrometer (Bruker Avance 400 MHz). Spectra were referenced internally to the residual proton resonance in CDCl_3 (δ 7.26 ppm). Chemical shifts (δ) were reported as part per million (ppm). ^{13}C NMR spectra were referenced to CDCl_3 (δ 77.16 ppm, the middle peak). Mass spectra (MS) were obtained on a Thermo Finnigan Surveyor MQS-plus mass spectrometer. ^1H -NMR, ^{13}C -NMR and MS spectra are provided in Supporting Information.

3. Results and Discussion

3.1 Cross-linked functional polymer (CFP) and immobilized metal nanoparticles

The three-dimensional copolymeric architectures (CFPs) are prepared through the copolymerization between 1, 3, 4, 6-tetraallylglycoluril and 4-vinyl pyridine. FTIR spectrum (Fig. S1) reveals that the materials are the copolymeric architectures of 4-vinyl pyridine and 1, 3, 4, 6-tetraallylglycoluril. 1598 cm^{-1} and 1471 cm^{-1} are skeleton vibration absorption peaks of six-member cycle of pyridine. 1700 cm^{-1} is the stretching vibration absorption peak attributed to a carbonyl group in glycoluril unit. 2927 cm^{-1} and 3022 cm^{-1} are stretching vibration absorption peaks of C-H bond. The weak peak of 1640 cm^{-1} is the stretching vibration absorption of unpolymerized double carbon-carbon bond. CFP begins to decompose at 308°C and ends at 440°C (thermal gravimetric analysis, Fig. S2). The average molecular weight and the distribution of CFP are determined by Gel Permeation Chromatography (GPC) (Fig. S3). Number-average molecular weight (M_n) is 13026 and weight-average molecular weight (M_w) is 39284. The polydispersity index (M_w/M_n) of CFP is 3.01. All chemical elements are detected by XPS survey spectrum of the copolymer of 4-vinyl pyridine and 1, 3, 4, 6-tetraallylglycoluril (Fig. S4).

The M_0 /CFP samples are illustrated in Scheme 1. The dispersion of metal nanoparticles and their chemical states are detailedly characterized by TEM, EDS, and XPS. The dispersion of Pt nanoparticles is revealed by TEM image (Fig. 1a). All nanoparticles are kept in the monodispersed state and the average size is about 2.0 nm. EDS of the selected region shows the presence of Pt species over the polymer. The

peaks of copper species are from the copper sample net. Fig. 1c shows Pt XPS peaks of the incipient metalated CFP. Pt species are unreduced and the binding energy of Pt 4f_{7/2} is 73.14 eV, which is indexed to the precursor (PtCl₄²⁻) [34]. After reduction with NaBH₄, the Pt XPS peaks are complicated. Fitting of the Pt 4f XPS envelope results in the identification of two chemical states of platinum: one with a binding energy of 72.2 eV with an atomic concentration of 52.4 % and another at 73.2 eV with an atomic concentration of 47.6 % (Fig. 1d). Pt 4f_{7/2} at the binding energy of 72.2 eV is attributed to zero-valent Pt nanoparticles. This value is about 1.0 eV higher than the binding energy of Pt 4f_{7/2} of bulk Pt metal. The size - effect of nanoparticles causes this difference. Pt 4f_{7/2} at the binding energy of 73.2 eV is attributed to unreduced PtCl₄²⁻ species. In the reduction process, the surplus amount of NaBH₄ and enough reaction time are applied.

Fig. 2a shows the dispersion of Pd nanoparticles over CFP. The average size of monodispersed Pd nanoparticles is about 4.5 nm. EDS of the selected region reveals the presence of Pd species (Fig. 2b). Fitting of the Pd 3d XPS envelope of the reduced Pd/CFP results in the identification of two chemical states of palladium: one with a binding energy of 334.9 eV, which is attributed to zero-valent Pd nanoparticles and another at 336.9 eV of Pd (II). The coexistence of Pd (0) and Pd (II) over the polymeric support occurs for the same reason as Pt/CFP.

As revealed by the TEM characterization, polymer-supported metal nanoparticles are mainly embedded in a swollen polymer matrix. Without a swelling agent, metal nanoparticles are tightly enclosed by the polymer framework and the interaction

between the reactants and the catalytic sites is impossible. (One sentence was deleted.)

The swollen polymer-supported catalyst contain temporary nanopores and mesopores than improve the accessibility of the catalytic active sites. The pores of the swollen CFPs have diameters in the order of nanometer (< 50 nm), which are suitable for technical application in catalysis. The as-synthesized Pt/CFP is tested in THF for hydrogenation of nitrobenzenes and two types of carbonylation of aryl iodide over CFP-supported Pd are performed in toluene or DMSO. The reaction solvents are good swelling agents for CFPs.

3.2 Hydrogenation of nitrobenzenes over Pt /CFP and carbonylation of aryl iodide over Pd /CFP

Hydrogenation is by far the most intensively investigated catalytic reactions. Platinum and palladium are generally harnessed as active metals. There are many comparative researches about metal catalysts supported on CFPs with those on traditional supports [25, 26]. Hydrogenation of nitrobenzenes is selected as the model reaction to investigate the catalytic performance of Pt/CFP, as listed in Table 1. (Two sentences were deleted.) Hydrogenation of nitrobenzene is performed under mild conditions. Commercial available Pt/C is used as the benchmark catalyst. Pt/CFP is more efficient than Pt/C when the metal amount of Pt/CFP is half of Pt/C. Total conversions of several nitrobenzenes are achieved with the substrate/Pt ratio of 4000 under low pressure of hydrogenation at room temperature. Substituent groups show little influence on the hydrogenation activity. Ortho-substituted substrate has some decrease in the final yield of hydrogenation product. The subtle relation between

microstructures of CFP-supported Pt nanoparticles and their catalytic performance will be investigated in the following section.

Carbonylation is a very important process for large-scale production of industrial chemicals: the carbonylation of methanol to acetic acid and the hydrocarbonylation of olefins to aldehydes. However, direct carbonylation with carbon monoxide attracts little attention in complex organic synthesis. Palladium-catalyzed carbonylation reactions of aromatic halides are rapidly-emerging carbonylative transformations to synthesize important intermediates (carboxylic acid derivatives, aldehydes, and ketones) in the manufacture of dyes, pharmaceuticals, agrochemicals, and other industrial products [35]. (One sentence was deleted.) The most employed catalysts are homogeneous palladium complexes. Heterogeneous catalysts are comparatively seldom considered. Actually, there are three inevitable problems to supported metal nanoparticle catalysts in carbonylation. First, the formation of metal carbonyl compound increases the mobility of metal nanoparticles during the reaction. Second, halide ions may lead to the deactivation of surfaces of metal nanoparticles. Third, strong base additives may cause the instability of the supporting materials. These problems are adverse factors of the recoverability and recyclability of supported metal nanoparticles. However, well-designed support microstructures and attachment strategy greatly mitigate the deteriorating trend during the catalytic conversion [36, 37].

Pd/CFP is used as the catalyst for carbonylation of iodobenzene in the presence of secondary amines. Double carbonylation competes with monocarbonylation. The

main reaction is the double carbonylation process (α -ketoamides). The double carbonylation of (hetero) aryl, alkenyl, and alkyl halides has been achieved in the presence of simple palladium complexes [38, 39]. To the best of our knowledge, the results in Table 2 are the newest discovery of double carbonylation of iodobenzenes over a heterogeneous palladium catalyst. Iodobenzene is totally converted and the yield of double carbonylation product nearly reaches 80%.

Iodide salts were proven to be promoters for the carbonylation process [40]. Several iodide salts were attempted to explore their promoting effects on double carbonylation (Fig. S5a). LiI is the best promoter with a dosage of approximately 5 mol% of iodobenzene. Increasing the adding amount of LiI causes marked loss of the selectivity to the double carbonylation (Fig. S5b).

The selectivity to α -ketoamide is related to the secondary amine. The carbonylation with hexamethylene imine shows the highest selectivity to α -ketoamides (Table 2). (One sentence was deleted.) In the carbonylation of iodobenzene, primary amines are not used as the nucleophiles because of the formation of imide [41]. For the carbonylation over Pd/CFP, the use of *n*-butylamine as the nucleophile results in the α -ketoamide selectivity of 65.8% and no imide products are detected in the final reaction mixture. The iodobenzenes with electron-withdrawing groups show lower activity in carbonylation and poor selectivity to double carbonylation products.

The scope of aminocarbonylation is extended by using acylhydrazines as the nucleophiles. The products of aminocarbonylation of acylhydrazines are important

precursors of pharmaceuticals and agrochemical [42]. The general method involves stoichiometric acyl chloride and leads to a large amount of acid and salt wastes. Carbonylation of aryl iodide with acylhydrazines is a green and efficient route to synthesize diacylhydrazines. The reaction conditions, including solvent, base, and reaction pressure, are detailedly screened (Table S1). Polar solvents are suitable for the aminocarbonylation of acylhydrazines and DMSO is the best solvent. DMF can be involved in the carbonylation and has a negative impact on the yield of target product [43]. When Cs_2CO_3 is used as the base, there is no carbonylation product. The use of organic bases, such as trialkylamines and N-heterocycle compounds, leads to the formation of the target products. Pyrazole and triethylamine are the two best bases (Table S1). (One sentence was deleted.) Because of the cost and post-treatment, triethylamine is selected as the base. Various substrates are tested in this reaction (Table 3). The product yields are in the range from 54.5% to 95.8%. (Two sentences were deleted.) A unique advantage of aminocarbonylation of acylhydrazines is the direct formation of diacylhydrazine with complex substituent groups. A selected iodobenzene molecule can be paired with a certain type of acylhydrazine to produce a well-designed diacylhydrazine molecule. As listed in Table 3, fourteen diacylhydrazine molecules are synthesized through the direct carbonylation over Pd/CFP.

3.3 The recyclability and recoverability of Pt /CFP in catalytic hydrogenation of nitrobenzene

The recyclability and recoverability of Pt/CFP in hydrogenation of nitrobenzene are

further investigated through a seven-run recycling test (Scheme 2). After the sixth recycling run, there is a marked decrease in the catalytic activity. (Three sentences were deleted.) XPS measurement reveals involvement and transformation of Pt nanoparticles in the catalytic cycle. After the fifth recycling test, the proportion of zero-valent Pt species decreases markedly (Fig. 3a, b). Fig. 3c shows the curve of Pt⁰/Pt²⁺ XPS intensity ratio's changes in each recycling run. The value decreases gradually after each recycling run. Spontaneous reduction of Pt (II) species is difficult to proceed under hydrogenation conditions. In our experimental observation, Pt (II)/CFP have very low activity in catalyzing hydrogenation of nitrobenzene and no Pt (0) species were detected after the treatment under hydrogenation conditions. The gradual transformation from Pt (0) to Pt (II) species directly leads to unrecoverable loss of catalytic activity.

For the fresh catalyst (Fig. 1a), Pt nanoparticles are kept in a uniform dispersion and their average size is approximately 1.4 nm. TEM image of the used catalyst after the fifth run shows some growth in size and their average size is 2.7 nm. The comparison between the particle density in Region 1 and that in Region 2 reveals the redispersion of Pt nanoparticles (Fig. S6) during the reaction process. The redispersion of Pt nanoparticles in CFP matrix is mainly attributed to the mobility of solutes and self-diffusion of solvents inside swollen CFPs under reaction conditions. (Two sentences were deleted.) Metal nanoparticles are inevitably involved in the catalytic cycles and their flexibility during the reaction determines the extent of activity regeneration after the reaction. Gradual size growth from 1.4 nm to 2.7 nm

and redispersion is another reason for unrecoverable loss of catalytic activity.

3.4 The flexibility of Pd /CFP during catalytic carbonylation of aryl iodide

As shown by the catalytic cycle of palladium-catalyzed double carbonylation of iodobenzenes (Scheme S1), palladium species are intensively involved in several key steps. Their transfer between the supported catalyst and the reaction solution is attributed to inevitably leaching of active metal species from palladium nanoparticles. (Two sentences were deleted.) The recyclability and recoverability of CFP-supported palladium nanoparticles are thoroughly investigated through a twelve-run recycling test of double carbonylation of iodobenzene in the presence of hexamethylene imine (Fig. 4). There are little fluctuations in the catalytic performance during the incipient six recycling runs. From the seventh to the twelfth recycling run, the conversion of iodobenzene is approximately 100% and the selectivity to the double carbonylation product increases gradually from 80.0% to 95.1%. After each test batch, the concentration of leaching palladium species in the reaction mixture is detected by ICP-OES. The leaching metal amount is negligible and shows no effect on the catalytic performance.

For supported palladium catalysts (complexes or nanoparticles), the leaching of palladium by the reaction flow is a serious problem [44, 45]. However, well-designed support structures and attachment strategy can efficiently immobilize the active centers and then greatly mitigate metal leaching during the catalytic conversion [36, 37]. (Two sentences were deleted.) The pyridine groups of CFPs could anchor and trap palladium carbonyl complexes from the catalytic cycle. The swollen copolymeric

gel phases of CFPs facilitate completing the entire carbonylation cycle inside the copolymeric architectures, and greatly mitigate the palladium leaching during mass transfer between the catalysts and the reaction solution.

The redispersion of palladium nanoparticles during the recycling test is characterized by TEM (Fig. S7a-d). (Two sentences were deleted.) With the recycling test proceeding, giant clusters of palladium nanoparticles are formed, but no agglomeration is observed. (One sentence was deleted.) The formation of giant clusters of palladium nanoparticles is attributed to swollen gel micro-phases in cross-linked polymer framework and molecular mobility and diffusion by the reaction flow [46]. The palladium species transfer among the nanoparticles in a certain form of palladium carbonyl intermediate, which can be trapped and decompose to generate new palladium nanoparticles. The palladium chemical states of the used catalyst (after the ninth recycling test) are detected by XPS (Fig. S7e). (One sentence was deleted.) The $3d_{5/2}$ peak at 335.1 eV is attributed to zero-valent palladium nanoparticles. Another $3d_{5/2}$ peak at 338.1 eV is indexed to Pd (II), which are trapped by functional sites over copolymeric architectures. The Pd⁰/Pd²⁺ XPS intensity ratio is calculated as 1.53. This value of the fresh catalyst is 0.78 (Fig. 2c). (Two sentences were deleted.) It has been demonstrated that Pd (0) species are active catalytic centers for double carbonylation [47]. The increase in their proportion has directly led to the improved selectivity to double carbonylation products, as shown in Fig. 4.

The hot filtration test is performed to directly define the metal leaching during the reaction [48]. Double carbonylation of iodobenzene in the presence of hexamethylene

imine is carried out for 4.0 h and then the reaction liquid mixture is drained into another autoclave through a stainless steel pipe with inter filter membrane. The hot reaction mixture without Pd/CFP is further stirred under typical CO pressure and temperature with newly added base (Fig. 5a). The amount of carbonylation products in the mixture is measured each hour in the sequent reaction period. No more products are formed and the carbonylation ceases. It is demonstrated that there are no leached palladium species in the reaction mixture, which are active in the carbonylation of iodobenzene. (Two sentences were deleted.) Double carbonylation of iodobenzene in the presence of hexamethylene imine is performed with $\text{PdCl}_2[\text{CH}_3\text{CN}]_2$ and blank CFP (Fig. 5b). In Region 1, the carbonylation shows a gradual increase in the yield of carbonylation products. In Region 2, the reaction is terminated and CFP is separated and cleaned. In Region 3, the separated CFP is used as the catalyst for iodobenzene carbonylation under the same reaction conditions as in Region 1. The separated CFP shows catalytic activity in the carbonylation and its TEM image (the insert in Fig. 5b) reveals the presence palladium nanoparticles over CFP. The blank CFP captures and traps active palladium carbonyl species, which in situ decompose to generate palladium nanoparticles.

(One paragraph was deleted.)

A five-run recycling test is carried out over Pd/CFP for aminocarbonylation of acylhydrazines (Scheme S2). We observe a marked loss of catalytic activity and leached palladium species in the reaction mixture after each test run (Scheme S3). TEM image of the used catalyst after the fifth run reveals that palladium nanoparticles

are transferred from CFP framework to the surface. (One sentence was deleted.) Pd/CFP is totally dissolved in DMSO under the reaction conditions and separated from the reaction mixture by adding diehtyl ehter. Products of aminocarbonylation of acylhydrazines are chelating ligands of palladium species. Their intensive involvement in the catalytic cycle facilitates leaching of palladium species with the reaction flow. The leaching of palladium species causes the loss of catalytic activity in the five-run recycling test.

4. Conclusions

In summary, 1, 3, 4, 6-tetraallylglycoluril was used as the cross-linker for preparing a cross-linked functional polymer with the monomer of 4-vinyl pyridine. Pt and Pd nanoparticles over the copolymeric support were introduced by the incipient metalation of the swollen polymeric framework with the precursors and the sequent reduction. Pt nanoparticles are kept in the monodispersed state and the average size is about 1.4 nm. The average size of monodispersed Pd nanoparticles is about 4.5 nm. Pt/CFP shows excellent catalytic performance in hydrogenation of nitrobenzenes under mild reaction reactions. Total conversions of several nitrobenzens are achieved with the substrate / Pt ratio of 4000 under low pressure of hydrogenation at room temperature. Pd/CFP is used as the catalyst for carbonylation of iodobenzene in the presence of secondary amines. The main reaction is the double carbonylation process (α -ketoamides) with the highest selectivity of 80%. A selected iodobenzene molecule can be paired with a certain type of acylhydrazine to produce a well-designed

diacylhydrazine molecule through the direct carbonylation over Pd/CFP. Supported Pt or Pd nanoparticles are intensively involved in the catalytic cycle. (One sentence was deleted.) The flexibility of metal nanoparticles and CFP supports guarantees macroscopic catalytic robustness. There are two main mechanisms for confining the irreversible transfer of metal nanoparticles: anchoring and trapping function of cross-linked functional copolymeric architectures and the presence of temporary nanopores and mesopores in the swollen CFP framework.

Acknowledgements

This work was financially supported by the National Natural Sciences Foundation of China (No. 21101161, 21174148, 21304101) and YMB New Energy Co.

Reference

- [1] B. Hammer, J. K. Nørskov, *Nature* 376 (1995) 238-240.
- [2] E. Roduner, *Nanoscope Materials: Size-dependent Phenomena*, The Royal Society of Chemistry, Cambridge, 2006, pp. 239-257.
- [3] C. R. Henry, in: U. Heiz U. Landman (Eds.), *Nanocatalysis*, Springer, New York, 2007, pp. 245-265.
- [4] S. Ferrero, A. Piednoir, C. R. Henry, *Nanoletters* 1 (2001) 227-230.
- [5] V. P. Zhdanov, B. Kasemo, *Phys. Rev. Lett.* 81 (1998) 2482-2495.
- [6] U. Heiz, A. Sanchez, S. Abbet, W. D. Schneider, *J. Am. Chem. Soc.* 121 (1999) 3214-3217.

- [7] S. Abbet, A. Sanchez, U. Heiz, W. D. Schneider, A. M. Ferrari, G. Pacchioni, N. Rosch, *J. Am. Chem. Soc.* 122 (2000) 3453-3457.
- [8] A. Roucoux, J. Schulz, H. Patin, *Chem. Rev.* 102 (2002) 3757-3778.
- [9] B. K. Min, C. M. Friend, *Chem. Rev.* 107 (2007) 2709-2724.
- [10] A. Acradi, *Chem. Rev.* 108 (2008) 3266-3325.
- [11] T. Risse, S. Shaikhutdinov, N. Nilius, M. Sterrer, H. J. Freund, *Acc. Chem. Res.* 41(2008) 949-956.
- [12] M. S. Chen, D. W. Goodman, *Chem. Soc. Rev.* 37 (2008) 1860-1870.
- [13] K. Lee, J. J. Zhang, H. J. Wang, D. P. Wilkinson, *J. Appl. Electrochem.* 36 (2006) 507-522.
- [14] A. Stein, *Adv. Mater.* 15 (2003) 763-775.
- [15] M. Kralik, A. Biffis, *J. Mol. Catal. A* 177 (2001) 113-138.
- [16] T. Akagi, M. Baba, M. Akashi, *Polymer* 48 (2007) 6729-6964.
- [17] Z. Huang, F. Li, B. Chen, F. Xue, G. Chen, G. Yuan, *Appl. Catal. A: General* 403 (2011) 104-111.
- [18] F. Li, B. Chen, Z. Huang, T. Lu, Y. Yuan, G. Yuan, *Green Chem.* 15 (2013) 1600-1607.
- [19] J. Wollner, W. Neier, *Bergbau und chemie (Homberg)*, German Patent 1260454, 1966.
- [20] D. Pears, S. C. Smith, *Aldrichimica Acta* 38 (2005) 23-33.
- [21] P. Centomo, M. Zecca, S. Lora, G. Vitulli, A. M. Caporusso, M. L. Tropeano, C. Milone, S. Galvagno, B. Corain, *J. Catal.* 229 (2005) 283-297.

- [22] B. Corain, K. Jerabek, P. Centomo, P. Canton, *Angew. Chem. Int. Ed.* 43 (2004) 959-962.
- [23] Y. Uozumi, R. Nakao, *Angew. Chem. Int. Ed.* 115 (2003) 204-207.
- [24] A. Biffis, A. Orlandi, B. Corain, *Adv. Mater.* 15 (2003) 1551-1555.
- [25] A. Biffis, B. Corain, Z. Cvengrosova, M. Hronec, K. Jerabek, M. Kralik, *Appl. Catal. A: General* 124 (1995) 355-365.
- [26] C. Burato, P. Centomo, G. Pace, M. Favaro, L. Prati, B. Corain, *J. Mol. Catal. A: Chem.* 238 (2005) 26-34.
- [27] M. Zecca, P. Centomo, B. Corain, in: B. Corain, G. Schmid, N. Toshima (Eds.), *Metal Nanoclusters in Catalysis and Materials Science: The Issue of Size Control*, Elsevier, Amsterdam, 2008, pp. 201-232.
- [28] R. Akiyama, S. Kobayashi, *Chem. Rev.* 109 (2009) 594-642.
- [29] K. Okamoto, R. Akiyama, H. Yoshida, T. Yoshida, S. Kobayashi, *J. Am. Chem. Soc.* 127 (2005) 2125-2135.
- [30] R. Akiyama, S. Kobayashi, *J. Am. Chem. Soc.* 125 (2003) 3412-3413.
- [31] Y. M. A. Yamada, S. M. Sarkar, Y. Uozumi, *J. Am. Chem. Soc.* 134 (2012) 3190-3198.
- [32] J. Lagona, P. Mukhopadhyay, S. Chakrabarti, L. Isaacs, *Angew. Chem. Int. Ed.* 44 (2005), 4844-4870.
- [33] A. Day, A. P. Arnold, R. J. Blanch, B. Snushall *J. Org. Chem.* 2001 (66), 8094-8100.

- [34] Y. M. Shul'ga, A. V. Bulatov, R. A. T. Gould, W. V. Konze, L. H. Pignolet, *Inorg. Chem.* 31 (1992) 4704-4076.
- [35] A. Brennfhrer, H. Neumann, M. Beller, *Angew. Chem. Int. Ed.* 48 (2009) 4114 – 4133.
- [36] A. J. Sandee, L. A. van der Veen, J. N. H. Reek, P. C. J. Kamer, M. Lutz, A. L. Spek, P. W. N. M. van Leeuwen, *Angew. Chem. Int. Ed.* 38 (1999) 3231-3235.
- [37] S. C. van der Slot, J. Duran, J. Luten, P. C. J. Kamer, P. W. N. M. van Leeuwen, *Organometallics* 21 (2002) 3873-3875.
- [38] Y. S. Lin, H. Alper, *Angew. Chem. Int. Ed.* 40 (2001) 779 – 781.
- [39] Y. Uozumi, T. Arii, T. Watanabe, *J. Org. Chem.* 66 (2001) 5272 – 5274.
- [40] Q. Xing, L. Shi, R. Lang, C. Xia, F. Li. *Chem. Commun.* 48 (2012) 11023-11025.
- [41] J. Balogh, A. Kuik, L. Urge, F. Darvas, J. Bakos, R. Skoda-Foldes, *J. Mol. Catal. A: Chem.* 302 (2009) 76-79.
- [42] J. Shang, Y. Liu, R. Huang, F. Bi, Q. Wang, *Heteroatom Chemistry* 18 (2007) 631-636.
- [43] A. Schnyder, M. Beller, G. Mehlretter, T. Nsenda, M. Studer, A. F. Indolese, *J. Org. Chem.* 66 (2001) 4311-4315.
- [44] V. Sans, F. Gelat, N. Karbass, M. I. Burguete, E. García-Verdugo, S. V. Luis, *Adv. Synth. Catal.* 352 (2010), 2851-2858.
- [45] M. I. Burguete, E. García-Verdugo, I. Garcia-Villar, F. Gelat, P. Licence, S. V. Luis, V. Sans, *J. Catal.* (2010) 269, 150-160.

- [46] H. Feld, A. Leute, D. Rading, and A. Benninghoven, *J. Am. Chem. Soc.* 112 (1990) 8166-8167.
- [47] R. M.B. Carrilho, M. M. Pereira, A. Takacs, L. Kollar, *Tetrahedron* 68 (2012) 204-207.
- [48] H. E. B. Lempers and R. A. Sheldon, *J. Catal.* 175 (1998) 62–69.

Scheme 1 The illustration of preparation procedure of cross-linked functional polymer supported metal nanoparticles.

Scheme 2 Seven-run recycling test of Pt/CFP for hydrogenation of nitrobenzene.

Fig. 1 a) TEM image of CFP supported Pt nanoparticles. b) EDS of the selected region. c) Pt XPS peaks of the unreduced Pt/CFP sample. d) Pt XPS peaks of the reduced Pt/CFP sample.

Fig. 2 a) TEM image of CFP supported Pd nanoparticles. b) EDS of the selected region. c) Comparison of Pd XPS peaks between the reduced Pd/CFP and the unreduced Pd/CFP.

Fig. 3 a) Pt XPS peaks of the fresh catalyst. b) Pt XPS peaks of the used catalyst after the fifth recycling test. c) The curve of Pt^0 / Pt^{2+} XPS intensity ratio's changes in each recycling run.

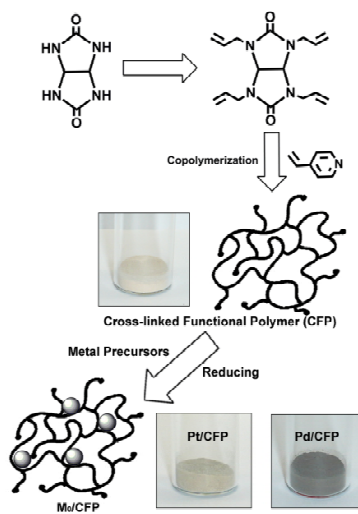
Fig. 4 The twelve-run recycling test of double carbonylation of iodobenzene in presence of hexamethylene imine over Pd/CFP.

Fig. 5 a) The hot filtration test of Pd/CFP for carbonylation of iodobenzene in the presence of hexamethylene imine. c) Carbonylation of iodobenzene in the presence of hexamethylene imine performed with $PdCl_2[CH_3CN]_2$ and blank CFP (the insert is TEM image of the used CFP).

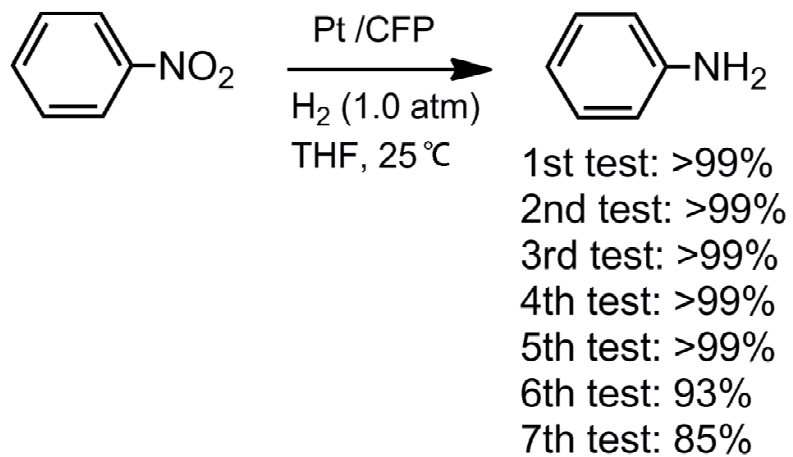
Table 1 Hydrogenation of nitrobenzenes over Pt/CFP.

Table 2 Carbonylation of aryl iodides in the presence of secondary amines.

Table 3 Carbonylation of aryl iodides in the presence of acylhydrazines.



Scheme 1 The illustration of preparation procedure of cross-linked functional polymer supported metal nanoparticles.



Scheme 2 Seven-run recycling test of Pt/CFP for hydrogenation of nitrobenzene.

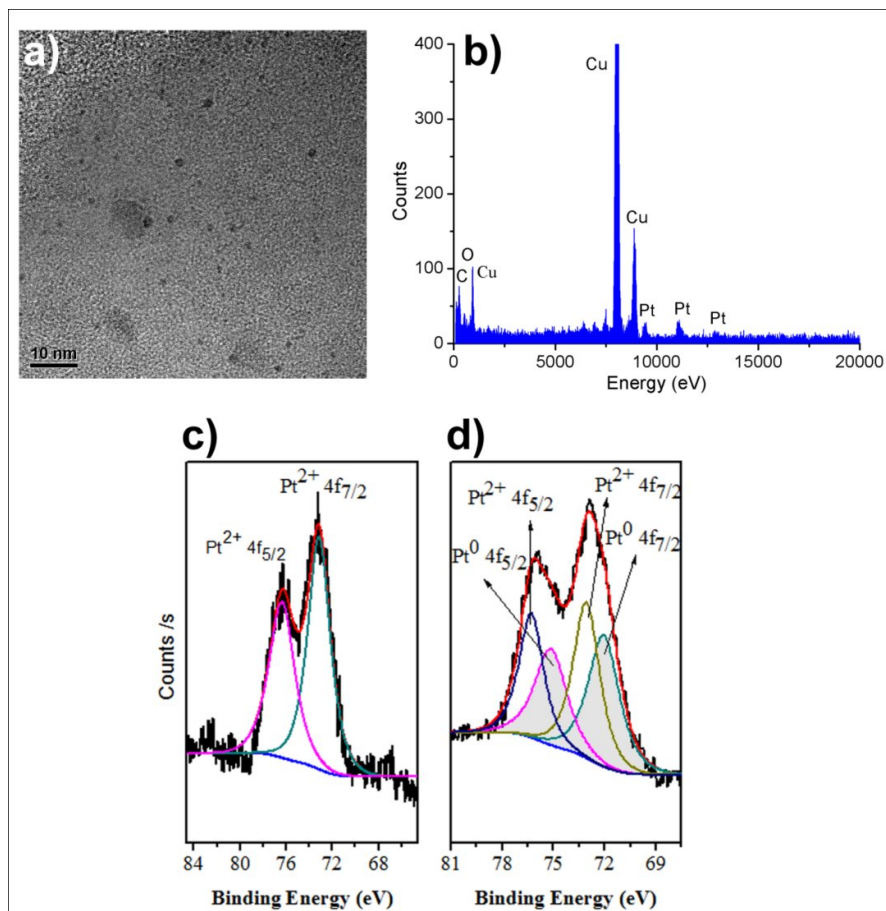


Fig. 1 a) TEM image of CFP supported Pt nanoparticles. b) EDS of the selected region. c) Pt XPS peaks of the unreduced Pt/CFP sample. d) Pt XPS peaks of the reduced Pt/CFP sample.

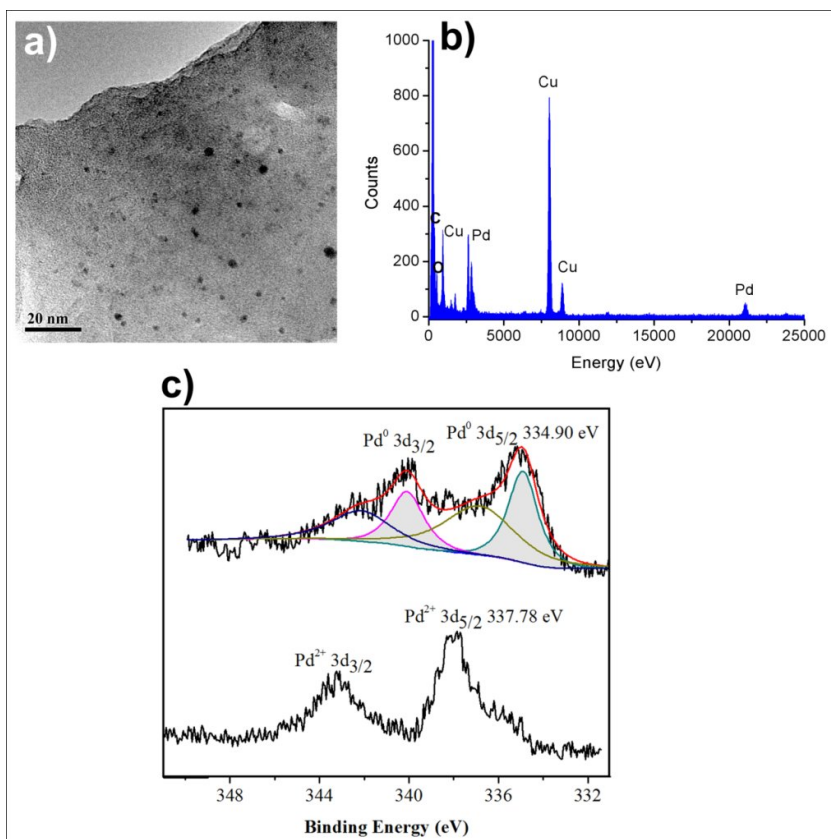


Fig. 2 a) TEM image of CFP supported Pd nanoparticles. b) EDS of the selected region. c) Comparison of Pd XPS peaks between the reduced Pd/CFP and the unreduced Pd/CFP.

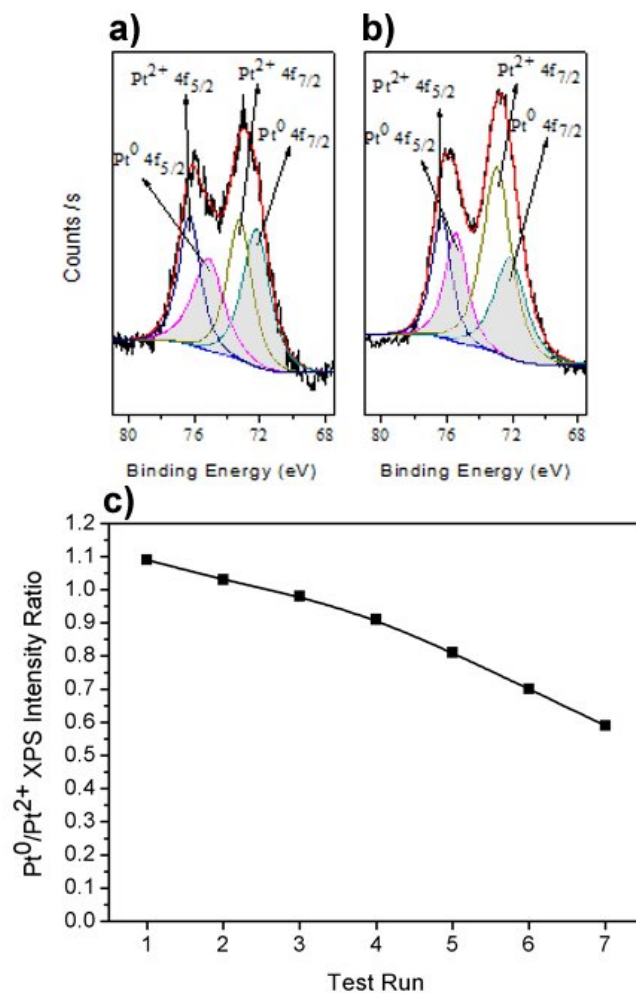


Fig. 3 a) Pt XPS peaks of the fresh catalyst. b) Pt XPS peaks of the used catalyst after the fifth recycling test. c) The curve of Pt⁰ / Pt²⁺ XPS intensity ratio's changes in each recycling run.

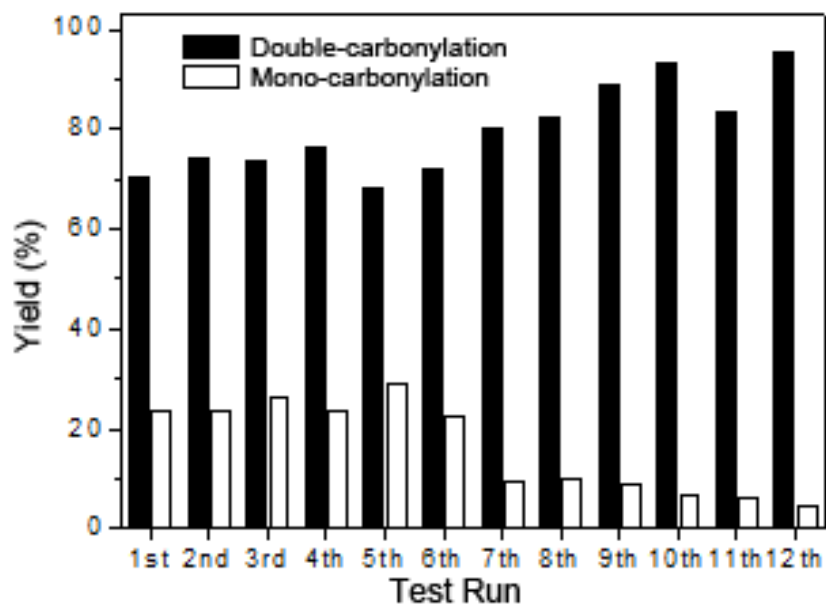


Fig. 4 The twelve-run recycling test of double carbonylation of iodobenzene in presence of hexamethylene imine over Pd/CFP.

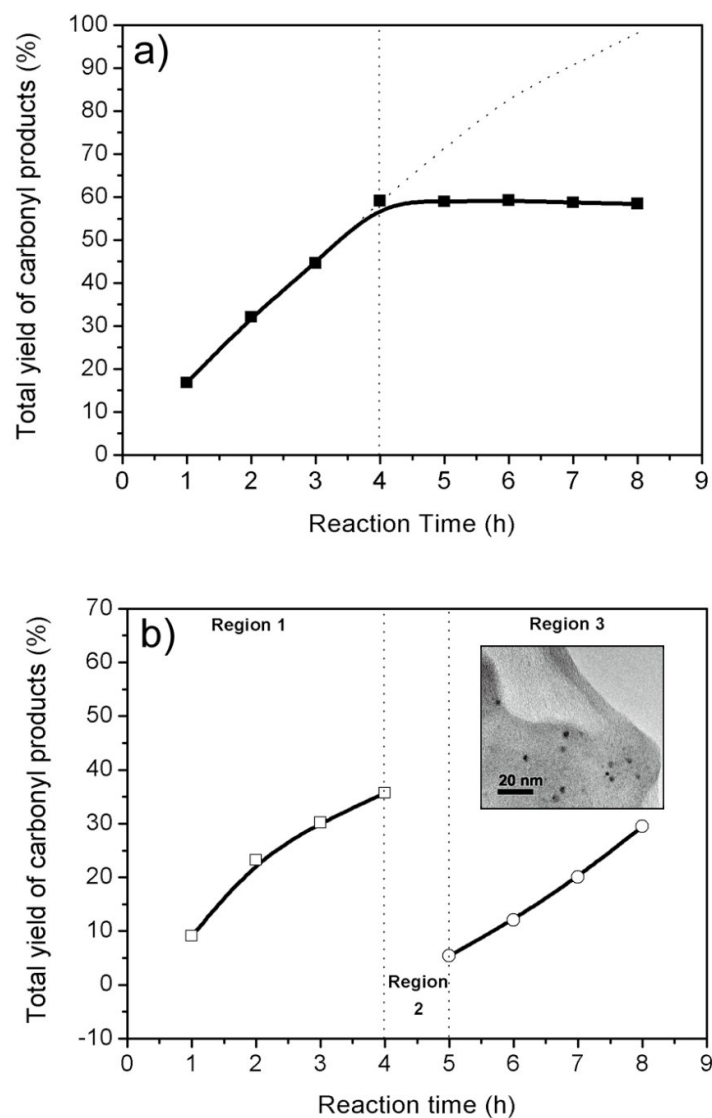
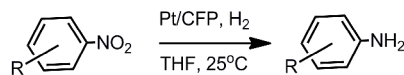
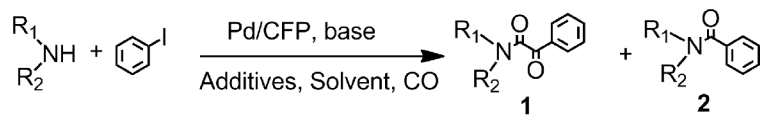


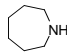
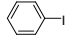
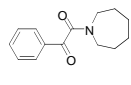
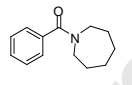
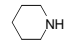
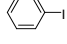
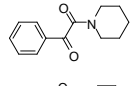
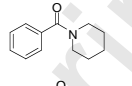
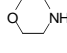
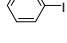
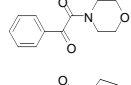
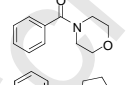
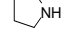
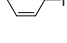
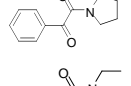
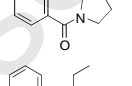
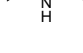
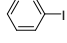
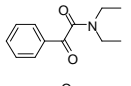
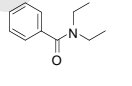
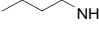
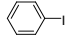
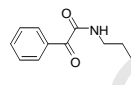
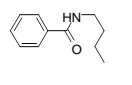
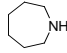
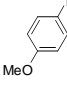
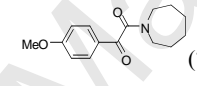
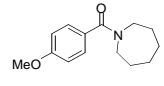
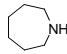
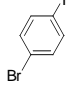
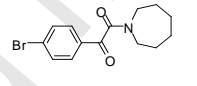
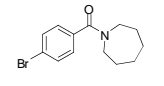
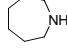
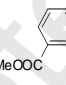
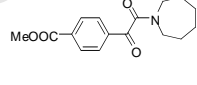
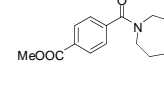
Fig. 5 a) The hot filtration test of Pd/CFP for carbonylation of iodobenzene in the presence of hexamethylene imine. c) Carbonylation of iodobenzene in the presence of hexamethylene imine performed with PdCl₂[CH₃CN]₂ and blank CFP (the insert is TEM image of the used CFP).

Table 1 Hydrogenation of nitrobenzenes over Pt/CFP

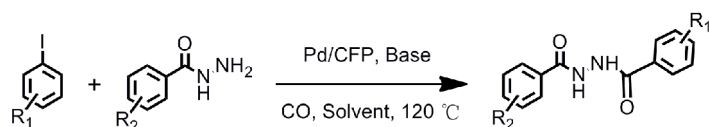
Entry	R	Catalyst (S/Pt) ^[a]	Reaction conditions	Yield (%) ^[b]
1	H	Pt/C (2000)	3 h, 25 \square , 1.0 atm H ₂	86
2	H	Pt/CFP (4000)	3 h, 25 \square , 1.0 atm H ₂	>99
3	4-methyl	Pt/CFP (4000)	3 h, 25 \square , 1.0 atm H ₂	>99
4	4-acetyl	Pt/CFP (4000)	3 h, 25 \square , 1.0 atm H ₂	>99
5	4-methoxyl	Pt/CFP (4000)	6 h, 25 \square , 1.0 atm H ₂	>99
6	2-hydroxyl	Pt/CFP (4000)	3 h, 25 \square , 1.0 atm H ₂	98

[a] S/Pt is the mole ratio of substrate to Pt, 1mmol substrate in 2 ml THF. [b] The value of hydrogenation yield is calculated from GC measurement results.

Table 2 Carbonylation of aryl iodides in the presence of secondary amines.

Entry	Amine	Aryl iodide	Product 1 yield (%) ^[a]	Product 2 yield (%) ^[b]
1			 (80)	 (18)
2			 (72)	 (22)
3			 (39)	 (37)
4			 (63)	 (26)
5			 (45)	 (13)
6			 (66)	 (23)
7			 (74)	 (26)
8			 (26)	 (36)
9			 (20)	 (40)

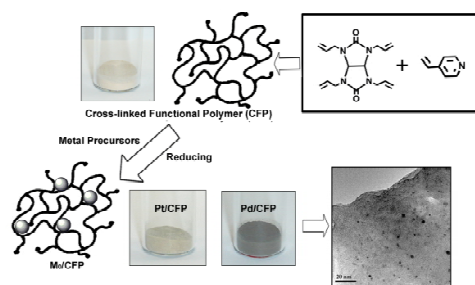
Reaction conditions: To a 100-ml autoclave, were added aryl iodide (1.0 mmol), secondary amine (5.0 mmol), the catalyst (Pd: 0.78 mol%), Cs₂CO₃ (1.14 g, 3.5 mmol), LiI (9.0 mg, 0.0479 mmol) and toluene (5.0 ml). The autoclave was flushed by CO flow and pressurized to 4.0 MPa. The reaction was performed at 120 °C for the given time. [a], [b]: the isolated yield.

Table 3 Carbonylation of aryl iodides in the presence of acylhydrazines

Entry	Substrate 1	Substrate 2	Product	Yield (%) ^[a]
1				95
2				93
3				90
4				76
5				76
6				88
7				91
8				96
9				72
10				66
11				73
12				55
13				75
14				67

Reaction conditions: To a 100-ml autoclave, were added aryl iodide (1.0 mmol), acylhydrazine (2.0 mmol), the catalyst (Pd: 0.78 mol%), base (1.06 mmol) and DMSO (5.0 ml). The autoclave was flushed by CO flow and pressurized to 4.0 MPa. The reaction was performed at 120 °C for the given time. [a] the isolated yield.

Graphic Abstract



Highlight

- A cross-linked functional polymer was prepared by 1, 3, 4, 6-tetraallylglycoluril.
- Pt/CFP shows excellent catalytic performance in hydrogenation of nitrobenzenes.
- The carbonylation of iodobenzene over Pd/CFP gives double-carbonylation products.
- Supported Pt and Pd nanoparticles show high macroscopic catalytic robustness.

Accepted Manuscript